Full-duplex-based Rate/Mode Adaptation Strategies for Wi-Fi/LTE-U Coexistence: A POMDP Approach

Mohammed Hirzallah, *Student Member, IEEE,* Wessam Afifi, *Student Member, IEEE,* and
Marwan Krunz, *Fellow, IEEE,*

Abstract—The rapid increase in wireless demand prompted the FCC to open up parts of the 5 GHz band for unlicensed access. This caught the interest of 4G/LTE providers, who wish to extend their LTE-A services to the unlicensed spectrum (LTE-U). In LTE-U, small-cell base stations aggregate unlicensed and licensed bands to increase the throughput. Wi-Fi/LTE-U coexistence is a challenging issue due to the different access mechanisms of these two systems, which may cause high collision rates and delays. By leveraging self-interference-suppression techniques, we propose joint mode/rate adaptation strategies for Wi-Fi/LTE-U coexistence. Specifically, a full-duplex enabled Wi-Fi station can transmit and receive data simultaneously (TR mode) to increase the throughput, or transmit and sense simultaneously (TS mode) to monitor the LTE-U activity. We model the LTE-U interference as a hidden Markov process, and solve the problem of jointly adapting Wi-Fi rates/modes using a framework of partially observable Markov decision process (POMDP). A detection approach based on the sliding window correlator is analyzed for the TS mode, which can differentiate between Wi-Fi and LTE-U signals. Our results indicate that our scheme provides 1.5x (1.9x) average throughput gain for Wi-Fi system in the low (high) SINR regime relative to a half-duplex-based scheme.

Index Terms—Wi-Fi/LTE-U coexistence, full-duplex, simultaneous transmission-sensing, HMM, POMDP, rate adaptation.

I. INTRODUCTION

The significant increase in the wireless demand prompted the FCC to open up parts of the 5 GHz Unlicensed National Information Infrastructure (U-NII) band for unlicensed access. This motivated wireless operators to extend their LTE-A services to the unlicensed spectrum (LTE-U). LTE-U exploits carrier aggregation to combine licensed and unlicensed spectrum, targeting higher downlink (DL) throughput for user equipments (UEs). Coexistence between heterogeneous systems such as LTE and Wi-Fi in the unlicensed band is particularly challenging due to the difference in their access mechanisms. In particular, Wi-Fi systems are contention based, whereas LTE/LTE-U systems are schedule based. Such heterogeneity makes coordination and interference management quite challenging, leading to higher collision rates, latency, and unfairness.

In an effort to reduce the impact of LTE-U on Wi-Fi, two approaches have been proposed: Carrier-sensing adaptive
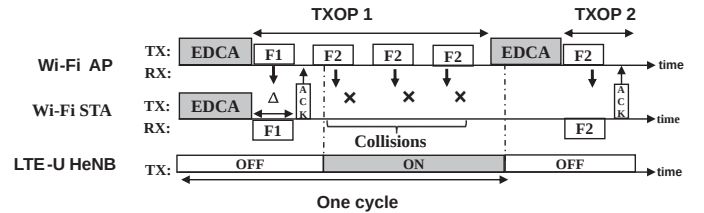
Fig. 1: Collision between LTE-U and Wi-Fi TXOP ('F1': Frame transmitted from AP).

transmission (CSAT) [1] and licensed assisted access (LAA) [2]. LAA, which was recently standardized in 3GPP Rel-13, targeted countries that mandate using listen-before-talk (LBT) in the 5 GHz band (e.g., Europe and Japan). A base station senses the spectrum and transmits if the measured signal is below −72 dBm. LAA transmissions may collide with Wi-Fi transmissions below this threshold. CSAT, which is advocated by the LTE-U Forum [3], relies on channel selection and time-based duty cycle (see Figure 1). The home eNodeB (HeNB) measures the traffic density of neighboring Wi-Fi stations (STAs) during the OFF period of the LTE-U system and adapts its duty cycle accordingly. In the ON period, HeNB transmits DL frames without performing LBT. On the other hand, Wi-Fi STAs can access the spectrum using the enhanced distributed channel access (EDCA) scheme, which is an extension of the distributed coordination function (DCF). The successful STA can reserve the channel for a duration called a transmit opportunity (TXOP), which may last for 3.008 ms. During a TXOP, a Wi-Fi access point (AP) or STA transmits several frames. After each frame, the AP/STA could wait for an ACK from its peer [4].

Deploying LTE-U small cells in unlicensed bands may lead to severe service degradation for Wi-Fi STAs. As shown in Figure 1, the AP detects a transmission failure (e.g., frame 'F2') via an ACK timeout. However, the AP cannot tell the reason for this transmission failure (e.g., channel fading and Wi-Fi/LTE-U interference). The AP may retransmit the corrupted frame several times. Once the retransmission limit is exceeded, the AP could either double its contention window size and back off again, or it could switch to a new channel. Both cases lead to performance degradation in terms of long delays, reduced throughput, and power wastage.

In this paper, we consider Wi-Fi devices with self-interference suppression (SIS) capabilities, which enable them to perform *simultaneous transmission and sensing* (TS). This so-called full-duplex *(FD) sensing* provides Wi-Fi STAs with

real-time channel monitoring and interference detection. Increasing the spectrum awareness at the AP helps it optimize its actions to maintain connectivity with the STAs. SIS techniques can also be used to enable *simultaneous transmission and reception* (TR) so as to increase the link throughput.

Wi-Fi standards (e.g., IEEE 802.11n/ac) define multiple modulation and coding schemes (MCSs), which can be used by the AP to adapt to channel dynamics, interference, and contention. We leverage this degree of freedom to jointly optimize the MCS and transmission "mode" at the AP, taking into account the AP's belief about LTE-U interference. Specifically, in addition to adapting its coding/modulation scheme, the AP can also select to operate in a TR or TS mode, or perform channel switching (CS).

FD sensing was previously explored for opportunistic spectrum access (OSA) systems, based on energy detection [5] and waveform-based detection [6]. Energy detection cannot differentiate between different types of signals (e.g., LTE-U vs. Wi-Fi). In contrast, waveform-based sensing uses training sequences, located in frame header to correlate. We harness the unique features of LTE-U and Wi-Fi signals (e.g., OFDM symbol duration and length of the cyclic prefix) to distinguish between the two. The authors in [7–9] exploited the cyclic prefix (CP) in OFDM symbols for signal detection, but only for HD systems (i.e., sensing only). In [7] the authors suggested a two-sliding-window approach, in which the received samples are correlated to detect the presence of OFDM symbols. We propose an FD sensing approach for coexisting Wi-Fi/LTE-U systems based on the two-sliding-window correlator scheme.

Several approaches for rate control have been proposed in the literature based on SNR measurements and MAC-layer statistics (see [10] and references therein). Generally, these approaches have slow response. Another approach is based on partially observable Markov decision processes (POMDP) [11–13], where the transmitter builds beliefs (probabilities) about the unknown channel conditions and uses them for selecting new rates. These works modeled the problem considering HD radios. In our scheme, we extend the POMDP framework and consider FD-enabled radios. We jointly control the FD mode and rate in response to LTE-U traffic dynamic. Interference generated by the LTE-U base station and received by Wi-Fi devices can be modeled as a hidden Markov model (HMM) process, and the joint rate/mode adaptation becomes a problem of HMM control, which can be solved within the framework of POMDPs [14]. The authors in [6] studied the problem of adapting the FD operation modes but with fixed MCSs, considering an OSA setting.

Previous work on LTE-U/Wi-Fi coexistence addressed different issues, ranging from evaluating the performance of coexisting systems through simulation/experimentation [15], to analyzing it using stochastic geometry [16]. The problem of channel selection for LTE-U cell has been analyzed in [17] usig a Q-learning approach. In [18] authors proposed an almost blank sub-frame scheme for enabling LTE in the unlicensed band. The proportional fair allocation for LTE and Wi-Fi has been derived in [19]. Achieving fair coexistence between LTE-U/LAA and Wi-Fi requires a comprehensive solution that integrates the optimal assignment for the clear channel assessment (CCA) thresholds, optimal channel access mechanisms, and efficient interference mitigation schemes. In this work, we focus on studying the interference mitigation aspect.

Our contributions are as follows. First, we propose an FD-enabled detection scheme for the TS mode based on the sliding window correlator (Section III). We derive the probabilities of detection and false-alarm under imperfect SIS, while taking into account inter-symbol interference (ISI). Second, we propose a modified TXOP scheme for Wi-Fi STAs with SIS capabilities (Section IV). In this scheme, Wi-Fi STAs exploit their SIS capabilities to either operate in the TS, TR, or CS modes. Third, we present a Markov model that incoporates the LTE-U ON/OFF activity (Section IV-A). Finally, we present a POMDP framework for determining the optimal Wi-Fi transmission strategy (FD mode and transmission rate) that maximizes the Wi-Fi link utility (Section V). We formulate the utility for different operation modes, rewarding the link for a successful transmission and penalizing it when outage occurs. In a preliminary version of this paper [20], we only discussed the sliding-window correlator detection scheme. Due to space limit, proofs of various results are omitted, but can be found in an online technical report [21].

II. System Model

We consider an LTE-U small cell that coexists with a Wi-Fi network in the unlicensed band (see Figure 2). The LTE-U small cell consists of an HeNB that communicates with a number of UEs over an aggregation of licensed and unlicensed channels. Without loss of generality, we focus on the LTE-U DL. The Wi-Fi system consists of one FD-enabled AP that communicates with a number of FD-enabled STAs. A Wi-Fi network implements an exclusive channel occupancy policy among its STAs. Specifically, a channel is allocated to only a single Wi-Fi. Contention is resolved using CSMA/CA, where neighboring STAs defer from accessing the channel by setting their network allocation vector (NAV) after decoding the duration field in the MAC header.

In LTE-U, the HeNB must search for a free channel to use. If no idle channel is found, HeNB shares the spectrum with the Wi-Fi system according to an adaptive duty cycle. During the OFF period, the HeNB measures the traffic intensity of neighboring Wi-Fi STAs (e.g., by recording the MAC addresses of overheard transmissions) and adapts its duty cycle accordingly.

Let $l(n)$, $s_a(n)$, $s_t(n)$, and $w(n)$, respectively, denote the LTE-U, Wi-Fi AP, Wi-Fi STA, and noise signals at sampling time n. We assume these signals follow a symmetric-circular-complex Gaussian distribution: $l \sim \mathcal{N}_c(0, \sigma_l^2)$, $s_a \sim \mathcal{N}_c(0, \sigma_s^2)$, $s_t \sim \mathcal{N}_c(0, \sigma_s^2)$, and $w \sim \mathcal{N}_c(0, \sigma_w^2)$. The received signals in the TR mode at the FD-enabled Wi-Fi AP is written as:

$$r_a(n) = \left(h_{la}(n) \otimes l(n)\right) + \left(h_{sa}(n) \otimes s_t(n)\right) + \left(\chi_a h_{aa} \otimes s_a(n)\right) + w(n) \qquad (1)$$

where $\otimes$ is the convolution operation, h_{la} is the channel gain between the HeNB and the Wi-Fi AP, h_{sa} is the channel gain between Wi-Fi STA and AP, respectively, h_{aa} is the gain
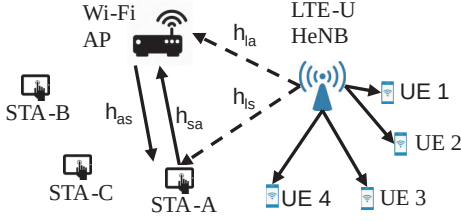
Fig. 2: System model of LTE-U/Wi-Fi coexistence (dashed lines represent interference from HeNB to Wi-Fi AP and STA).

Fig. 3: Sliding-window-based OFDM signal detector.

Fig. 4: $M_\tau(n)$ vs. $n/(N+L)$.　　Fig. 5: $M_\tau(n)$ vs. $\tau/(N+L)$.

of the self-interference channel of the AP (the attenuation between its transmit and receive chains), and χ_a is the SIS factor of the AP (perfect SIS occurs when $\chi_a = 0$). LTE-U interfering signal traverses multiple paths and suffers ISI before reaching the AP. We introduce the following three metrics: ISI to noise ratio (ISNR), residual self-interference to noise ratio (STNR), and the interference-to-noise ratio (INR). The ISNR $= \beta^2 |h_{la}|^2 \sigma_{\tilde{l}}^2/\sigma_w^2$ quantifies the ISI relative to the noise floor, where $\sigma_{\tilde{l}}^2$ is the power of the previously received LTE-U symbol. The STNR $= \chi_a^2 |h_{aa}|^2 \sigma_s^2/\sigma_w^2$ quantifies the AP residual self interference power relative to the noise floor. We focus on the LTE-U signal detection problem at the AP. The INR $= \sigma_l^2 |h_{la}|^2/\sigma_w^2$ indicates LTE-U signal level with respect to the AP noise floor. The signal-to-noise ratio (SNR) is SNR $= |h_{sa}|^2 \sigma_s^2/\sigma_w^2$. The signal-to-interference-and-noise (SINR) ratio for the AP is written as (a similar quantity can be defined for the STA):

$$\text{SINR} = \frac{|h_{sa}|^2 \sigma_s^2}{|h_{la}|^2 \sigma_l^2 + \chi_a^2 |h_{aa}|^2 \sigma_s^2 + \sigma_w^2} = \frac{\text{SNR}}{\text{INR+STNR+1}} \quad (2)$$

III. CYCLIC-PREFIX-BASED DETECTION

Differentiating between different types of interference helps the AP tune its mode/rate based on the detected interference type and maximize its utility. LTE-U and Wi-Fi signals are OFDM based, with every OFDM symbol consisting of a sequence of data symbols and a CP that is appended to the start of the data symbol (see Figure 3). This CP is a replication of some data symbols. It is added for several purposes, including time guarding and facilitating synchronization and decoding at OFDM receivers. CP is most likely to be contaminated by ISI.

Consider an LTE-U OFDM symbol that consists of N data samples and L CP samples. At the Wi-Fi receiver, the received analog signal is passed through the analog-to-digital converter (ADC) to obtain discrete samples. We buffer these samples and assign them to two windows, W_1 and W_2, where the timing difference between these windows equals $(N-L)\delta_n$; δ_n being the duration of a sample. The two windows are swept over all received samples (see Figure 3), where samples in these windows are correlated and compared against a certain detection threshold. We propose the following correlation timing metric:

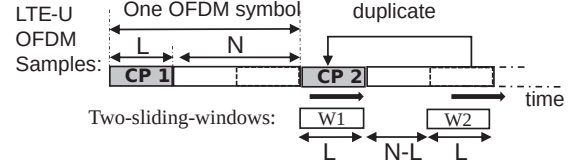$$M_\tau(n) = \frac{|A(n)|^2}{(\max(E_1(n), E_2(n)))^2} \quad (3)$$
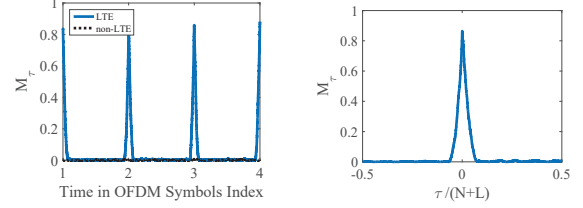
where $A(n)$ is the correlation between corresponding samples in the two windows, and $E_1(n)$ and $E_2(n)$ are the energies of the samples in the two windows, respectively:

$$A(n) = \sum_{k=0}^{L-1} r_a(n-k) r_a^*(n-k-N) \quad (4)$$

$$E_1(n) = \sum_{k=0}^{L-1} r_a(n-k-N) r_a^*(n-k-N), \quad E_2(n) = \sum_{k=0}^{L-1} r_a(n-k) r_a^*(n-k)$$

where $*$ is complex conjugate. We refer to the time instant at which the samples in the two windows correspond to the CP and its original duplicated part as the *optimal time*. The optimal time indicates the presence of an LTE-U signal, where the correlation value exceeds a certain threshold. For other time instances (called *regular times*), the correlation value will be small. In the absence of an LTE-U signal, the correlation value will also be small. The index τ in M_τ indicates the alignment of the sliding windows with respect to OFDM symbol's starting point (i.e, CP). τ takes integer values in the period $(-(N+L)/2, (N+L)/2]$, with $\tau = 0$ corresponding to the optimal time and $\tau > L$ corresponding to regular times. Figure 4 shows $M_\tau(n)$ as a function of the OFDM symbol index when four symbols are detected. Figure 5 depicts $M_\tau(n)$ vs. τ. Both figures are generated with INR = 25 dB, $L = 500$, $N = 6400$, and ISNR = 6 dB.

We define the hypothesis testing as follows:

$$r_a(n) = \begin{cases} \chi_a s_a(n) + w(n), & \text{under } \mathcal{H}_0 \text{ , HeNB is OFF} \\ l(n) + \chi_a s_a(n) + w(n), & \text{under } \mathcal{H}_0, n \text{ is a regular time} \\ l(n) + \chi_a s_a(n) + w(n), & \text{under } \mathcal{H}_1, n \text{ is the optimal time} \end{cases}$$
$$(5)$$

where the first two lines in (5) represent the null hypotheses $\mathcal{H}_0$, and the third line represents the alternate hypothesis $\mathcal{H}_1$. Define the general detection rule as follows:

$$\tilde{\delta}(r_a(n)) = \begin{cases} 1 & \text{if } M_\tau(n) \geq \lambda_{th} \\ 0 & \text{if } M_\tau(n) < \lambda_{th} \end{cases} \quad (6)$$

where λ_{th} is the detection threshold (determined next). We derive the statistics of $M_\tau(n)$ at the optimal time, regular times, and in the absence of LTE-U signals in our technical report [21].

Proposition 1. *At the optimal time, the distribution of M_τ can be approximated as a normal distribution of mean $\mu_{M_{\tau=0}} = \mu_Q^2$*
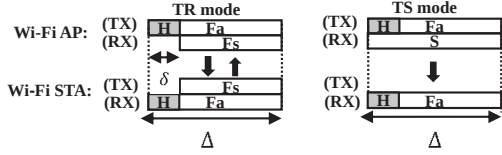
Fig. 6: FD modes: TR and TS modes ('S': Sense, 'Fa': AP frame, 'Fs': STA frame, and 'H': Header).
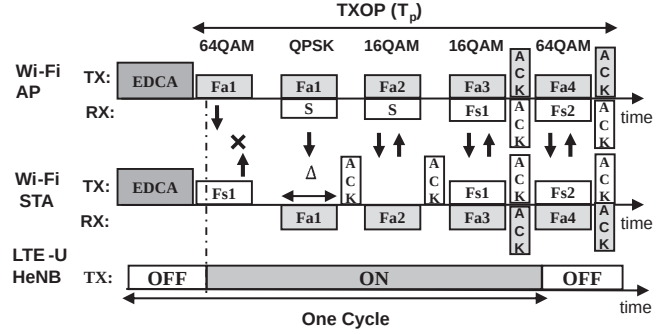

Fig. 7: Example of a modified TXOP operation mode ('S': Sense, 'Fa1', 'Fa2', 'Fa3', 'Fa4': Frames sent by AP, and 'Fs1', 'Fs2': Frames sent by STA).

and variance $\sigma^2_{M_{\tau=0}} = 4\mu^2_Q \sigma^2_Q$, where μ_Q and σ^2_Q are defined [21].

Proposition 2. *At any regular time, the distribution $M_{\tau>L}$ can be approximated by a gamma distribution $\Gamma(\frac{k}{2}, 2a_1)$, where $k/2 = 1$ is the shape parameter and $2a_1 = \frac{2L}{(L+0.7978\sqrt{L})^2}$ is the scale parameter.*

Proposition 3. *In the absence of an LTE-U signal, the distribution of M_τ (denoted as M_0) can be also approximated by gamma distribution $\Gamma(\frac{k}{2}, 2a_1)$.*

Note that $M_\tau(n)$ has the same distribution at regular times and in the absence of an LTE-U signal. The probability of detection at a threshold λ_{th} is:

$$P_d(\lambda_{th}) = \Pr\left[\{M_{\tau=0} \geq \lambda_{th}|\mathcal{H}_1\}\right] = Q\left(\frac{\lambda_{th}-\mu_{M_{\tau=0}}}{\sigma_{M_{\tau=0}}}\right) \quad (7)$$

where $Q(\cdot)$ is the complementary cumulative function of the standard normal distribution. The false-alarm probability is given by:

$$P_F(\lambda_{th}) = \Pr[\{M_0 > \lambda_{th}\}|\mathcal{H}_0] = 1 - F_{\gamma,1,2a_1}(\lambda_{th}) \quad (8)$$

where $F_{\gamma,1,2a_1}(\lambda_{th})$ is the CDF of a gamma distribution with shape parameter one and scale parameter $2a_1$. The proofs for the above results can be found in [21].

A. Neyman-Person (NP) Detection

We propose an NP detection rule based on the previously derived statistics. Note that false-alarms occur when there is no LTE-U signal and also at *regular times*. Let the maximum acceptable false-alarm probability be α. The NP detection threshold λ_{th} in (6) is:

$$\lambda_{th} = \lambda_{NP} = F^{-1}_{\gamma,1,2a_1}(1-\alpha). \quad (9)$$

The NP detector does not require any prior knowledge of the signal nor noise statistics; it only requires knowing the CP length. Note also that the sensing outcomes are independent of what technology LTE uses in the unlicensed band (i.e., CSAT or LAA). The two-sliding-window correlator has a low computational complexity and small memory overhead. This sensing scheme opens the way for adapting Wi-Fi CCA thresholds in response to CSAT/LAA activities, where more sensitive energy detection thresholds can be assigned. Due to space limit we leave this issue to future investigations.

IV. MODIFIED WI-FI TXOP

We now propose a modified TXOP scheme for FD-enabled Wi-Fi systems. We divide the TXOP into N_p time slots of

equal duration, during which AP and STA can exchange UL and DL frames. We consider two FD modes: The simultaneous Transmit-Receive (TR) mode and the simultaneous Transmit-Sense (TS) mode, as shown in Figure 6. Wi-Fi AP switches between these modes to mitigate the interference caused by LTE-U transmission. We assume that the AP is the session "master". It instructs the STA about the recommended mode of operation (e.g., TR or TS) and the associated MCS indices that the STA has to use by embedding this information in the DL frame's optional header field (e.g., field 'H' in Figure). This information requires a few bits, and hence represents small overhead. When LTE-U interference is relatively high the Wi-Fi AP has an option of quitting the TXOP period early and switching to a new channel. We use CS to refer to this channel-switching mode. AP also has the option of backing off until LTE-U completes transmission and the channel becomes idle again.

In the TR mode, the transmitted DL and UL frames can have different MCS indices (e.g., k_D and k_U, respectively). The Wi-Fi STA first reads the 'H' field in the DL frame and extracts the mode/MCS indices. Next, STA initiates a simultaneous UL transmission with MCS index k_U. After transmitting DL and UL frames, the AP and STA have to exchange ACK frames in both directions, indicating successful reception. In the TS mode, the AP sends a DL frame with an MCS index k_D, and simultaneously senses for any LTE-U signal using the detection scheme introduced in Section III. At the end of each time slot, AP updates its belief about LTE-U HeNB interference, and selects a new FD mode with suitable MCS indices for the next time slot (as discussed in Section V).

An example of the proposed TXOP scheme is shown in Figure 7, where the AP sends five DL frames (e.g., $N_p = 5$), each of duration Δ. In this example, the AP starts in the TR mode with MCS indices $k_D = k_U$, whose modulation is 64QAM. AP sends in the DL direction frame 'Fa1'. STA reads the header field and starts transmitting the 'Fs1' frame in the UL direction using 64QAM modulation. HeNB ON cycle starts just after the start of 'Fa1' and 'Fs1' transmission, which causes collision. Both AP and STA are not able to decode their received frames, and hence no ACKs are transmitted. In this case, the AP updates its belief about HeNB interference and selects a new action (as explained in Section V). For instance,

the next optimal action might be retransmitting the 'Fa1' frame in the TS mode with QPSK modulation. If STA is able to decode this frame, it will send back an ACK. Upon receiving an ACK for 'Fa1' and sensing an HeNB signal, the AP updates its belief about HeNB interference and may decide to raise the modulation to 16QAM with TS mode for the next transmitted frame (e.g., frame 'Fa2'). The process continues as shown in Figure 7. In order for the AP to select the optimal action, which maximizes the link utility in the TXOP period, it should be able to quantify the amount of LTE interference that the AP and STA receive. This interference is affected by the channel gains between AP/STA and HeNB. We model LTE activity and its interference using a FSMC model.

A. Finite-State Markov Channel (FSMC) Model

We assume that h_{la} and h_{ls} are block Rayleigh fading channels with Doppler frequency f_d, so these channels maintain a fixed level of fading over a time slot (e.g., Δ). Conventional FSMC models are based on paritioning the SINR variations into a set of nonoverlapping regions, in which the SINR remains in one region for a certain period of time. SINR changes only from one region to adjacent ones. We divide h_{la} and h_{ls} channel gains into M states, where state $s^{(i)}$, $i = 1, \cdots, M$, represents the i-th SINR region (i.e., $s^{(i)} = \{\zeta : g_i \leq \zeta < g_{i+1}\}$), where g_i and g_{i+1} are region's boundaries. We assign these boundary thresholds according to the supported MCS indices, as explained in Subsection IV-B. For a Rayleigh fading channel with average SINR $\bar{\zeta}$, the steady-state probabilities of these M states can be computed as $\epsilon_i = \Pr(\zeta \in s^{(i)}) = \int_{g_i}^{g_{i+1}} \frac{1}{\bar{\zeta}} \exp^{-\frac{z}{\bar{\zeta}}} dz$ [22].

Let $\tilde{p}_{i,j}$ be the transition probability between the ith and jth states, $i, j \in \{1, 2, \ldots, M\}$. These $\tilde{p}_{i,j}$'s can be expressed as a function of the level crossing rate (LCR), steady state probabilities, and average fade duration. LCR indicates the rate at which the signal across the threshold g_i. It can be written as $L_{g_i} = \sqrt{\frac{2\pi g_i}{\bar{\zeta}}} f_d \exp\{-\frac{g_i}{\bar{\zeta}}\}$. By averaging L_{g_i} by the time the channel remains in state $s^{(i)}$ (i.e., average fade duration ϵ_i/Δ), we can approximate $\tilde{p}_{i,i+1}$ and $\tilde{p}_{i,i-1}$ as follows:

$$\tilde{p}_{i,i+1} \approx L_{g_{i+1}}\Delta/\epsilon_i, \text{ for } i = 1, \cdots, M-1$$
$$\tilde{p}_{i,i-1} \approx L_{g_i}\Delta/\epsilon_i, \text{ for } i = 2, \cdots, M$$
$$\tilde{p}_{i,i} = 1 - \tilde{p}_{i,i+1} - \tilde{p}_{i,i-1}, \text{ for } i = 2, \cdots, M-1 \quad (10)$$

while $\tilde{p}_{1,1} = 1 - \tilde{p}_{1,2}$ and $\tilde{p}_{M,M} = 1 - \tilde{p}_{M,M-1}$.

This FSMC model does not account for LTE dynamics (i.e., it assumes that HeNB is always ON). In CSAT/LAA[1], HeNB alternates between ON and OFF states. Let X_{ON} and X_{OFF} be the distribution for these periods, with means $\bar{x}_{ON}$ and $\bar{x}_{OFF}$. Wi-Fi AP could estimate these distributions and their means through measurements and parametric estimation. We first define a simple Markov chain with two states, then we explain how to use it for modulating the previous FSMC. Let t_0 be the time instant the HeNB has been sensed switching OFF. Let t_1 be the time instant when AP starts the TXOP. Let ℓ be the index of the time slot in TXOP, where $\ell = \{1, \cdots, N_p\}$.

Let $u_{11,\ell}$ denotes the probability that the HeNB remains OFF for a period of Δ seconds starting at time $t_1 + (\ell - 1)\Delta$. Let $u_{12,\ell}$ be the probability that HeNB switches from OFF to ON during the ℓth time slot. The transition probabilities, $u_{11,\ell}, u_{12,\ell}$ can be defined as follows:

$$u_{11,\ell} = \frac{1 - F_{X_{OFF}}(t_1 - t_o + \ell\Delta)}{1 - F_{X_{OFF}}(t_1 - t_o + (\ell - 1)\Delta)}, \quad u_{12,\ell} = 1 - u_{11,\ell}$$

where $F_{X_{OFF}}(\cdot)$ is the CDF of X_{OFF}. The steady state probabilities of this OFF state can be evaluated as $\epsilon_{OFF} = \bar{x}_{OFF}/(\bar{x}_{ON} + \bar{x}_{OFF})$ [23]. We scale the transition probabilities in (10), and define new FSMC transition probabilities. Let $\hat{p}_{i,j}$ denotes the probability of transition from state $s^{(i)}$ to state $s^{(j)}$, then the transition probabilities for the new FSMC are:

$$\hat{p}_{i,j} = u_{11,\ell}\tilde{p}_{i,j}, \quad \forall \tilde{p}_{i,j} \neq 0, \forall i \leq M - 2$$
$$\hat{p}_{i,j} = u_{12,\ell}/(M - i - 1), \quad \forall j > i + 1, \forall i \leq M - 2$$
$$\hat{p}_{i,j} = \tilde{p}_{ij}, \quad i > M - 2$$
$$\hat{p}_{i,j} = 0, \quad \text{otherwise} \quad (11)$$

As we will explain in Section V, Wi-Fi AP takes decisions based on its belief about h_{la} and h_{ls} channel gains. We extend the FSMC model to account jointly for these channels. We introduce a two-dimensional Markov chain based on the transition probabilities defined in (11). Let $p_{im,jn}$ denotes the transition probabilities for which channels h_{la} and h_{ls} switch from states i to j and from states m to n, respectively. The state transitions for channel h_{la} and h_{ls} are independent. Accordingly, $p_{im,jn}$ can be stated as follows:

$$p_{im,jn} = \hat{p}_{i,j}\hat{p}_{m,n}, \forall i, j, m, n = 1, \cdots, M. \quad (12)$$

B. SINR Threshold Selection

IEEE 802.11 standards assign various MCSs with convolutional coding and low-density parity-check (LDPC) codes. Let $\mathcal{K}$ denotes the set of supported MCSs, where $\mathcal{K} = \{k : 0, \cdots, |\mathcal{K}| - 1\}$. IEEE 802.11ac standards specify the *relative constellation error*[2] (RCE) values for every MCS index. The RCE is a measure of how far constellation points are from their true locations, and it is defined as a root-mean-square (RMS) of the normalized difference between the power of the true and deviated constellation points. Constellation points deviate their true locations due to many reasons, including hardware impairments (e.g., noise and frequency offsets), interference, and channel impairments such as fading. RCE and SINR are related according to $RCE_{rms} \approx \sqrt{1/SINR}$ [24]. We assign the SINR thresholds for the $M = |\mathcal{K}| + 1$ states according to the supported MCSs. Let $INR_{th,k}$ denotes the maximum LTE-U interference to noise ratio where Wi-Fi transmission with MCS index k still supported, then $INR_{th,k} = 2(RCE_{k,rms}) + SNR - STNR$, where $RCE_{k,rms}$ is the maximum RCE_{rms} supports the kth MCS. The fading boundaries in the FSMC model are assigned as $g_{j+1} = INR_{th,k=M-j-1}$, while the lower and upper thresholds are $g_1 = 0$ and $g_{M+1} = \infty$, respectively. Let $\theta_k^{(i)}$ be

---

[1]LAA can be modeled as an ON/OFF process, because of the "discontinuous transmission" functionality imposed by regulation.

[2]RCE is known also as error vector magnitude (EVM).

the outage function indicator for the kth MCS index when the channel gain is in the ith state, then

$$\theta_k^{(i)} = \begin{cases} 1 & \text{, for } \mathrm{INR}^{(i)} > \mathrm{INR}_{\mathrm{th},k}, \ \forall k \in \mathcal{K} \\ 0 & \text{, otherwise.} \end{cases} \quad (13)$$

where $\mathrm{INR}^{(i)}$ denotes the actual INR of LTE-U signal (i.e., $\mathrm{INR}^{(i)} \in [g_i, g_{i+1})$). $\theta_k^{(i)} = 1$ indicates that the Wi-Fi transmission is unsuccessful.

V. DECISION THEORETIC FRAMEWORK FOR TRANSMISSION MODE/RATE CONTROL

Wi-Fi AP mitigates the interference caused by LTE-U transmissions by jointly adapting FD modes and transmission rates during the TXOP period. This requires the knowledge of h_{la}, h_{ls}, h_{as}, and h_{sa} channel gains. The channel gains of h_{as} and h_{sa} can be implicitly and explicitly estimated. However, the HeNB cannot estimate the h_{la} and h_{ls} channel gains, because Wi-Fi and LTE-U uses different techologies. Wi-Fi AP can still obtain partial knowledge about these channel gains by monitoring the performance of Wi-Fi UL and DL links over time. For example, AP can indirectly deduce interference levels through monitoring ACKs and decoding received frames during TXOP period. Therefore, AP has to jointly control rates/modes in response to LTE-U hidden processes using this partial knowledge. This motivates the need for a HMM control scheme which can be formulated through a POMDP framework [14]. POMDP assigns a belief (probability) for each unknown parameter, and updates this belief sequentially over time based on the resultant outcomes. POMDP maximizes the Wi-Fi utility through mapping its belief about the LTE-U interference to a set of actions, consisting of recommended joint rate/mode configurations. This mapping function is also known as the policy of POMDP.

For simplicity, we assume that channels between Wi-Fi AP and STA (i.e., h_{as} and h_{sa}) are static, and focus on formulating the POMDP problem for the channels between LTE-U HeNB and Wi-Fi nodes (i.e., h_{la} and h_{ls}). First, we introduce the main components needed for formulating the POMDP problem. Then, we introduce the reward functions and explain the policy evaluation.

a) Time Horizon: POMDP will take place over a finite horizon equals to the duration of one TXOP period (i.e., T_p second), where a total of $N_p = T_p/\Delta$ frames have to be exchanged each of Δ duration. In other word, there will be N_p time slots during each TXOP transmission. We denote each time slot as $\ell \in \{1, \cdots, N_p\}$.

b) State Space: The state space represents the status of h_{la} and h_{ls} channel gains. We model the state space according to the FSMC model that is presented in Subsection IV-A. We introduce a two dimensional finite state space $\mathcal{S}: M \times M$, where each state corresponds to h_{la} and h_{ls} channel gains. The number of states per each channel is $M = |\mathcal{K}| + 1$. We denote the $(h_{la}^{(i)}, h_{ls}^{(m)})$ state as $s^{(i,m)} \in \mathcal{S}$.

c) Action Space: At the start of each time slot, Wi-Fi AP has to take two decisions simultaneously; the FD mode (e.g., TR, TS, or CS) and the applicable transmission rates (i.e., the MCS indices k_U and k_D for the UL and DL transmissions,

respectively). The channel switching CS mode is only selected when the transmission with the lowest MCS index is believed to be unsuccessful; given that AP has enough knowledge about suitable channels for switching to. AP could also replace the CS action by a 'backoff' action, where it backs off until LTE-U gets OFF and channel becomes idle again. The action space is written as $\mathcal{A} = \{\mathrm{TR}\,(k_D, k_U), \mathrm{TS}\,(k_D), \mathrm{CS}\}$, and it has $|\mathcal{K}|^2 + |\mathcal{K}| + 1$ possible actions. We denote the action that the AP takes at the start of time slot ℓ as a_ℓ.

d) Observation Space: Wi-Fi AP takes an action $a_\ell \in \mathcal{A}$ at the start of time slot ℓ and waits for an observation at the end. This observation depends on the action that the AP takes and the true state of interference. The AP takes a TR action and receives four possible observations: Decode or Undecode $\{D, U\}$ for the UL frame and ACK or NACK $\{A, N\}$ for the DL frame. At the end of a TS action, Wi-Fi AP receives four possible outcomes: ACK or NACK for the DL frame and busy B or idle I for the sensing. The observation space is written as $O = \{\{\bar{o}_{\mathrm{TR}}\}, \{\bar{o}_{\mathrm{TS}}\}\}$, where $\bar{o}_{\mathrm{TR}} \in \{(D, A), (D, N), (U, A), (U, N)\}$, and $\bar{o}_{\mathrm{TS}} \in \{(I, A), (I, N), (B, A), (B, N)\}$. Let $\bar{o}_\ell$ denotes the observation vector that AP receives at the end of time slot ℓ. Let $q_{a_\ell, \bar{o}_\ell}^{(i,m)}$ denotes the probability of receiving an observation vector $\bar{o}_\ell$ when the AP takes an action a_ℓ, while the channel states are $(h_{la}, h_{ls}) = (i, m)$:

$$q_{\mathrm{TR}\,(k_D, k_U), \bar{o}_{\mathrm{TR}}}^{(i,m)} = \begin{cases} (1 - \theta_{k_U}^{(i)})(1 - \theta_{k_D}^{(m)}), & \text{for } \bar{o}_{\mathrm{TR}} = (D, A) \\ (1 - \theta_{k_U}^{(i)})\,\theta_{k_D}^{(m)} & \text{, for } \bar{o}_{\mathrm{TR}} = (D, N) \\ \theta_{k_U}^{(i)}\,(1 - \theta_{k_D}^{(m)}) & \text{, for } \bar{o}_{\mathrm{TR}} = (U, A) \\ \theta_{k_U}^{(i)}\,\theta_{k_D}^{(m)} & \text{, for } \bar{o}_{\mathrm{TR}} = (U, N) \end{cases}$$

$$q_{\mathrm{TS}\,(k_D), \bar{o}_{\mathrm{TS}}}^{(i,m)} = \begin{cases} (1 - \mathrm{P_d^{(i)}})(1 - \theta_{k_D}^{(m)}), & \text{for } \bar{o}_{\mathrm{TS}} = (I, A) \\ (1 - \mathrm{P_d^{(i)}})\,\theta_{k_D}^{(m)} & \text{, for } \bar{o}_{\mathrm{TS}} = (I, N) \\ \mathrm{P_d^{(i)}}\,(1 - \theta_{k_D}^{(m)}) & \text{, for } \bar{o}_{\mathrm{TS}} = (B, A) \\ \mathrm{P_d^{(i)}}\,\theta_{k_D}^{(m)} & \text{, for } \bar{o}_{\mathrm{TS}} = (B, N) \end{cases}$$

where $\theta_{k_U}^{(i)}$ and $\theta_{k_D}^{(m)}$ are the outage indicator functions defined in (13) and $\mathrm{P_d^{(i)}}$ is the detection probability of LTE-U/LAA signal as in (7).

e) Belief Updates: Wi-Fi AP maintains a belief about the actual status of h_{la} and h_{ls} channel gains. Let $\bar{\pi}_\ell \in \mathcal{B}$ be the AP's belief vector about the M^2 states at the start of the time slot ℓ, where $\mathcal{B}$ denotes the belief space. The AP takes an action $a_\ell \in \mathcal{A}$, monitors an observation $\bar{o}_\ell \in O$, and updates its belief vector for the next coming time slot $\ell + 1$ according to the following Bayes rule ($\pi_{\ell+1}^{(j,n)} = T_{a_\ell, \bar{o}_\ell, \bar{\pi}_\ell}^{(j,n)}$):

$$T_{a_\ell, \bar{o}_\ell, \bar{\pi}_\ell}^{(j,n)} = \frac{q_{a_\ell, \bar{o}_\ell}^{(j,n)} \sum_{i=1}^{M} \sum_{m=1}^{M} p_{im,jn} \pi_\ell^{(i,m)}}{\sum_{j'=1}^{M} \sum_{n'=1}^{M} q_{a_\ell, \bar{o}_\ell}^{(j',n')} \left(\sum_{i=1}^{M} \sum_{m=1}^{M} p_{im,j'n'} \pi_\ell^{(i,m)} \right)} \quad (14)$$

where $\pi_{\ell+1}^{(i,m)}$ is an element in $\bar{\pi}_{\ell+1}$. The belief vector will be helpful for derving the POMDP policy, because is has been proved to be a sufficient statistic [25].

A. Utility Formulation

Let the DL and UL frames consist of d_{dl} and d_{ul} data symbols, where each frame lasts for a time period of Δ

seconds. The UL and DL frame rates, namely, $R_{DL}^{k_D}$ and $R_{UL}^{k_U}$, respectively, are written as:

$$R_{DL}^{k_D} = d_{dl} b_{k_D} c_{k_D} / \Delta, \qquad R_{UL}^{k_U} = d_{ul} b_{k_U} c_{k_U} / \Delta \qquad (15)$$

where $b_{k_D}, c_{k_D}, b_{k_U}$, and c_{k_U} are the modulation order and coding rate for the DL and UL frames, respectively. Let P_a and P_s denotes the power consumed in the AP and STA frame transmissions, respectively. We define the utility function $W_{a_\ell, \bar{o}_\ell}$ for actions and observations at the ℓ time slot as:

$$W_{TR\,(k_D, k_U), \bar{o}_\ell} = \begin{cases} R_{UL}^{k_U} + R_{DL}^{k_D} - \eta P_a - \eta P_s & , \bar{o}_\ell = (D, A) \\ R_{UL}^{k_U} - \eta P_a - \eta P_s & , \bar{o}_\ell = (D, N) \\ R_{DL}^{k_D} - \eta P_a - \eta P_s & , \bar{o}_\ell = (U, A) \\ -\eta(P_a + P_s) & , \bar{o}_\ell = (U, N) \end{cases}$$

$$W_{TS\,(k_D), \bar{o}_\ell} = \begin{cases} R_{DL}^{k_D} - \eta P_a & , \bar{o}_\ell = (I, A) \\ -\eta P_a & , \bar{o}_\ell = (I, N) \\ R_{DL}^{k_D} + \Gamma^{k_D} - \eta P_a & , \bar{o}_\ell = (B, A) \\ \Gamma^{k_D} - \eta P_a & , \bar{o}_\ell = (B, N) \end{cases}$$

$$W_{CS, \bar{o}_\ell} = \eta(P_a + P_s) \qquad (16)$$

where η is a scaling coefficient used to match power and rate terms and Γ^{k_D} is the *awareness reward* constant, which is used to reward the AP for detecting the LTE-U signal when it is ON. We reward the AP for taking the TS action only when LTE-U is ON. Γ^{k_D} and η are left as implementation parameters.

B. POMDP Problem Solution

The AP updates its belief vector as in (14), and takes an action based on a pre-defined policy. This policy is a function μ that maps the belief vector $\bar{\pi}_\ell$ to an action $a_\ell \in \mathcal{A}$ (i.e., $\mu : \bar{\pi}_\ell \mapsto a_\ell$). The optimal policy μ^* is the one that maximizes the expected reward over the TXOP period. At time slot ℓ, the AP incurs an immediate reward (a.k.a. myopic reward) for each action a_ℓ it takes. This action also has an expected long term reward on future (e.g., slots $\ell + 1$ to N_p) (a.k.a. reward-to-go). AP's expected reward is the sum of these two rewards, and it is formulated using the value function $V_{a_\ell}(\bar{\pi}_\ell)$. The optimal policy μ^* is a sequence of actions that maximizes this value function over the TXOP period. The immediate reward for an action a_ℓ taken at the start of time slot ℓ is defined as:

$$D_{a_\ell}(\bar{\pi}_\ell) = \sum_{\bar{o}_\ell \in O} \sum_{i=1}^{M} \sum_{m=1}^{M} \pi_\ell^{(i,m)} q_{a_\ell, \bar{o}_\ell}^{(i,m)} W_{a_\ell, \bar{o}_\ell}. \qquad (17)$$

We plot the immediate reward as a function of LTE-U interference in Subsection VI-B2. The long term reward for an action a_ℓ taken at time slot ℓ is defined as:

$$L_{a_\ell}(\bar{\pi}_\ell) = \kappa \sum_{\bar{o}_\ell \in O} \left\{ \left(\max_{a'_{\ell+1} \in \mathcal{A}} V_{a'_{\ell+1}}(\bar{\pi}_{\ell+1}) \right) \Lambda_{a_\ell, \bar{o}_\ell, \bar{\pi}_\ell} \right\} \qquad (18)$$

where $\Lambda_{a_\ell, \bar{o}_\ell, \bar{\pi}_\ell}$ is the denominator in (14) and κ is a discount factor that prioritizes the long term reward, $\kappa \in [0, 1]$. Notice that the $\max_{a'_{\ell+1} \in \mathcal{A}} V_{a'_{\ell+1}}(\bar{\pi}_{\ell+1})$ term is the optimal value function

at time slot $\ell + 1$. Consequently, the value function of taking action a_ℓ at time slot ℓ can be formulated by combining the immediate reward (17) and the long term reward (18):

$$V_{a_\ell}(\bar{\pi}_\ell) = D_{a_\ell}(\bar{\pi}_\ell) + \kappa L_{a_\ell}(\bar{\pi}_\ell). \qquad (19)$$

The optimal policy at time slot ℓ can be derived as:

$$\mu^*(\bar{\pi}_\ell) = \arg \max_{a_\ell \in \mathcal{A}} V_{a_\ell}(\bar{\pi}_\ell). \qquad (20)$$

The value function in (19) has been proved to be a piecewise linear and convex [25]. The domain in (20) is the belief space $\mathcal{B}$, which is a continuous space. Obtaining the optimal solution for POMDP is computationally feasible for small number of system states (e.g., up to 10 states). The number of states in our system is much larger, and accordingly sub-optimal or approximate solutions are preferable. Lots of algorithms have been proposed in literature for approximating the solution for POMDPs with large number of state [26, 27]. We have solved the above problem using SARSOP, a point-based approximate POMDP solver [28]. SARSOP reduces the complexity of (19) by sampling a subset of the belief space $\mathcal{R} \subset \mathcal{B}$, and solving the problem in (20) successively. SARSOP updates $\mathcal{R}$ based on a simple online learning technique.

VI. PERFORMANCE EVALUATION

A. Sliding Window Correlator

We consider an FD enabled Wi-Fi STA with noise floor $\sigma_w^2 = -90$ dBm, and transmitted power $\sigma_s^2 = 20$ dBm. We set $\sigma_{\tilde{I}}^2 = \sigma_w^2$ and vary σ_I^2, β, and χ_a. We analyze how different SIS capabilities, and ISI contamination in the CP affect detector's performance for various setups using numerical and simulation results. We set $L = 500$ and $N = 6400$ taking into account the sampling frequency used in typical Wi-Fi receivers $f_s \geq 20$ MHz and the time length of an LTE-U OFDM symbol (e.g., $72\mu sec$). Unless otherwise stated, all simulation results were generated with 3000 realizations.

In Figures 8 and 9, we set the false alarm probability to 0.01 and compute the NP detection threshold as in (9). Next, we evaluate the mis-detection probability through simulation and numerical computations as derived in (7). The detection scheme attains the 10^{-3} mis-detection probability at even low LTE-U signal level such as INR = -5 dB (see the 'No ISI' plots in Figure 8). Detector performance degrades as more ISI and residual self interference are generated.

We analyze the receiver operating characteristic (ROC) performance of the developed detector for several INR, ISI, and SIS conditions (see Figures 10, 11 and 12). We notice an increase in the false alarm probability as LTE-U signal level decreases below a certain limit (see the 'INR = -1 dB' plot in Figure 10). Similar result also holds for ISI and self interference; the false alarm probability increases as STNR increases beyond a certain limit (see the 'STNR = 10 dB' plot in Figure 12 and the 'ISNR = 2 dB' plot in Figure 11).

B. Joint Rate and Mode Adaptation Scheme

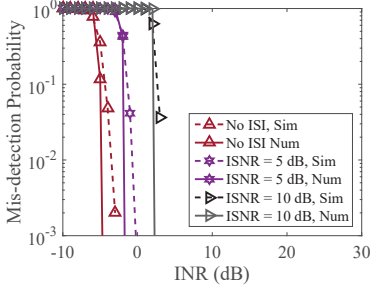*1) Simulation Setup and Methodology:* We start with a simple topology consisting of a Wi-Fi pair (e.g., AP and

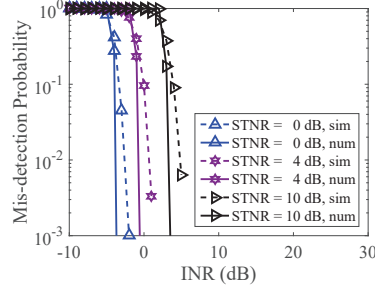Fig. 8: Mis-detection probability vs. INR for various ISI levels ($P_F = 0.01$, no RSI).

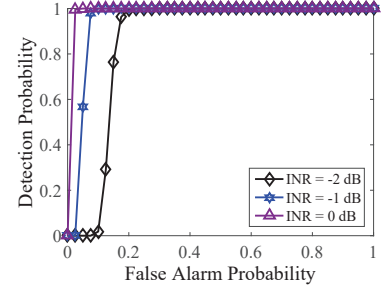Fig. 9: Mis-detection probability vs. INR for various RSI (P_F=0.01, ISNR=2 dB).

Fig. 10: ROC curves for various INR levels (ISNR = 2 dB, STNR = 5 dB).
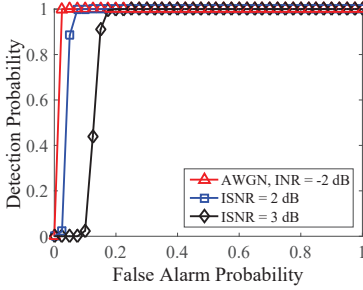

Fig. 11: ROC curves for various ISI levels (INR = −2 dB, STNR = 2 dB).
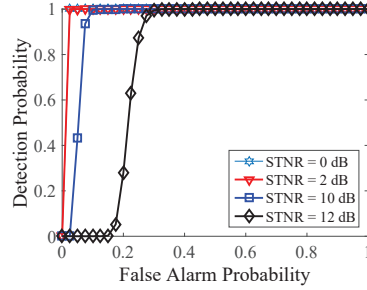

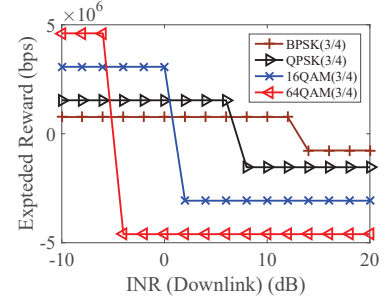Fig. 12: ROC curves for various RSI levels (ISNR = 2 dB, INR = 2 dB).

Fig. 13: TS mode reward vs. INR at the DL (SNR = 25 dB, STNR = 5 dB).

STA) that coexists with one LTE-U small cell. The two systems share a channel of 20 MHz in an indoor environment. We have set channel parameters according to the technical reports [2, 3]. We assume that both Wi-Fi and LTE-U have saturated traffic. We assume that Wi-Fi AP has contended successfully for a channel access, and occupies the spectrum for a duration equals to the TXOP maximum period (i.e., 3 msec). We simulate various SINR scenarios by varying the location of the Wi-Fi STA and evaluating the achieved throughput for each scenario. We set the SINR at AP and STA receiver to be equal. Initially, we set LTE-U ON and OFF periods to be exponentially distributed with equal means of 10 msec, and then we relax these values. We consider the following MCS indices $\mathcal{K} = \{0, \cdots, 7\}$ with the corresponding modulation orders $b_k \in \{1, 1, 2, 2, 4, 4, 6, 6\}$ and coding rates $c_k \in \{1/2, 3/4, 1/2, 3/4, 1/2, 3/4, 2/2, 3/4\}$. We compare the performance of our proposed joint rate/mode (JRM) adaptation scheme against the following adaptation schemes. (*i*) The optimal (OPT) adaptation scheme: Wi-Fi AP has a full knowledge about actual interference and SINR values at the AP and STA receivers. OPT scheme has an oracle knowledge and attains the capacity of the FD channel. (*ii*) Single MCS stepping (SMS) adaptation scheme: Wi-Fi AP steps up and down the used MCS index in response to the success and failure of the previous frame transmissions, respectively. SMS scheme emulates other rate adaptation schemes proposed in literature, including adaptive rate fallback (ARF), but is has a faster response [10]. In the third scheme, we consider a fixed FD mode TR with a fixed MCS-k (TFM-k).

2) Immediate Reward Plots: The performance of the TS expected immediate reward function $D_{a_\ell = \text{TS}(k_D)}$ defined in (17) is shown in Figure 13 for various MCS indices.

These plots represent the upper bound of the expected reward. The associated MCS index in the DL transmission scales as desired. Lower MCS indices become more desirable as INR increases in the DL. We also plot the immediate expected reward function defined in (17) for TR mode $D_{a_\ell = TR(k_D, k_U)}$ versus the LTE-U interference received by the STA for various MCS indices, as shown in Figure 14. We see that by increasing the INR in the DL transmission the recommended MCS index reduces as desired.

3) Wi-Fi Performance: We study the performance of the proposed JRM scheme in comparison with TFM-k scheme (see Figure 15). JRM scheme scales with the changes in SINR. The overall average performance for the proposed scheme outperforms the fixed MCS assignment. This proves the importance of adapting the rate for mitigating LTE-U interference.

Classical WLAN rate adaptation schemes, namely, Onoe, ARF/AARF, and SampleRate have relatively slow response; they adapt MCS indices every tens, hundreds, or thousands of msec [10]. Our scheme adapts the rate on a shorter time scale. The SMS scheme mimics these classical schemes and has a faster response. We compare the performance for our scheme against the SMS scheme in Figure 16. JRM scheme outperforms the SMS because it adapts for interference while taking into account LTE-U behavior, while SMS adapts the rate in an ad hoc fashion. We investigate the performance of JRM scheme when compared with OPT scheme(see 'OPT-FD' and 'OPT-HD' plots). 'OPT-FD' and 'OPT-HD' plots represent the upper bounds that the AP can achieve for the FD and HD cases, respectively. JRM provides 1.5x to 1.9x throughput gain relative to the OPT-HD.
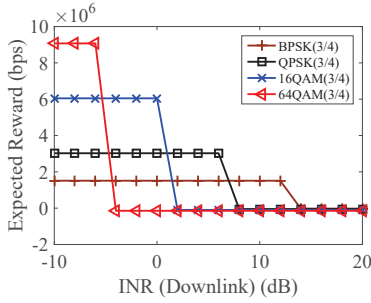
Fig. 14: TR mode reward vs. INR at the DL (UL INR = 2 dB, $k_D = k_U$).
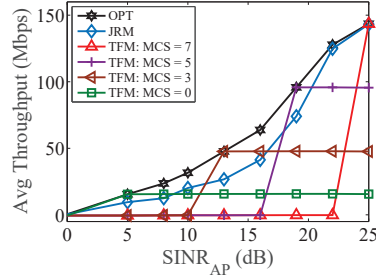

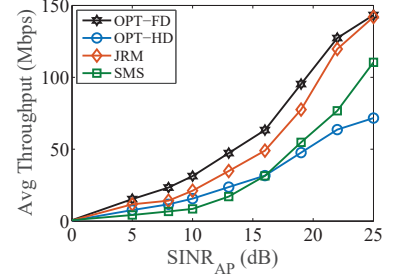Fig. 15: Wi-Fi average throughput vs. SINR at AP.

Fig. 16: Wi-Fi average throughput vs. SINR at AP for various adaptation schemes.
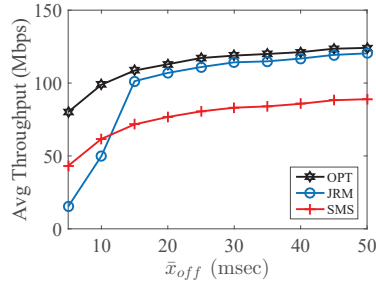

Fig. 17: Wi-Fi average throughput vs. LTE-U OFF period mean (exponentially distributed).
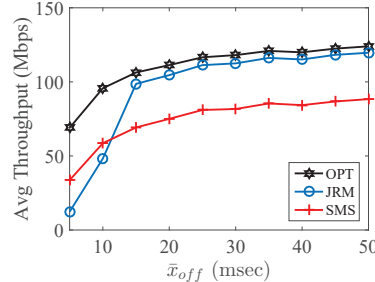

Fig. 18: Wi-Fi average throughput vs. LTE-U OFF period mean (uniformly distributed).
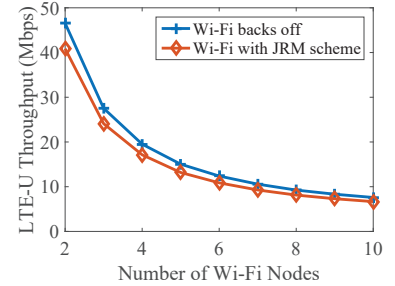

Fig. 19: LTE-U throughput vs. the number of Wi-Fi nodes.

4) Wi-Fi Performance and LTE-U Behavior: Our scheme is a ware of LTE-U behavior, which is enabled with the help of the two-sliding-windows sensing scheme. Sensing provides the AP with an improved awareness about LTE-U activities. Accordingly, the AP adapts operation by selecting modes and rates based on the POMDP policy. We illustrate how different LTE-U parameters trigger POMDP adaptation. In particular, we model LTE-U with an ON/OFF process for which ON and OFF periods can be exponentially and uniformly distributed. We fix the mean for the ON period to 10 msec, and vary the mean for the OFF period accordingly. Generally speaking, this setup mimics the behavior of LAA and CSAT. We plot the Wi-Fi AP average throughput versus the mean of the OFF period when it is exponentially distributed (see Figure 17) and uniformly distributed (see Figure 18). There are three observations to read from these plots. As expected, we notice that the increase in the mean of the OFF period enhances the performance of Wi-Fi. We also notice that JRM scheme outperforms SMS scheme and approaches the OPT scheme. SMS has relatively a slight increase in the achieved throughput, but this increase saturates early because SMS scheme is agnostic about LTE-U behavior. On the other hand, we notice that JRM scheme approaches the OPT scheme as the mean of the OFF period exceeds that of the ON period.

5) LTE-U Performance: In our scheme, Wi-Fi AP does not back off in response to collisions caused by LTE-U. Instead, Wi-Fi AP mitigates collisions by jointly adapting rate and mode. We seek to analyze how this behavior might impact LTE-U performance. Let's consider a simple CSAT duty cycle adaptation scheme for which the HeNB adapts the duty cycle according to the number of Wi-Fi nodes (e.g., $d_c = 1/(n+1)$)

We set LTE-U ON and OFF period to be 20 msec and gen-erate uniformly random Wi-Fi transmission attempts during LTE-U OFF period, where each Wi-Fi transmission lasts for 3 msec. Figure 19 shows that Wi-Fi collisions causes relatively minimal degradation to LTE-U performance.

VII. CONCLUSIONS

Wi-Fi/LTE-U coexistence faces many challenges due to the dissimilarities between LTE-U and Wi-Fi technologies. In this work, we addressed two problems: The detection of LTE-U signal and the adaptation of Wi-Fi modes/rates assuming an FD framework. We have introduced an FD-based sliding-window correlator that detects LTE-U signals, and analyzed the detector performance under imperfect self-interference suppression. We have also harnessed our detection scheme for mitigating the LTE-U interference. We have introduced a POMDP-based adaptation scheme for jointly adapting Wi-Fi FD modes and transmission rate (i.e., MCS indices). Our results indicate that joint rate and mode adaptation provides on average around 1.5x at low SINR and 1.9x at high SINR throughput gain over the maximum HD theoretical throughput. Future work includes considering the coexistence between several LTE small cells and Wi-Fi networks.

REFERENCES

[1] LTE-U Forum, "LTE-U CSAT procedure TS v1.0," , Oct. 2015.
[2] 3GPP, "Study on licensed-assisted access to unlicensed spectrum," 3GPP TR. 36.889 v13.0.0., June. 2015.
[3] LTE-U Forum, "LTE-U SDL coexistence specfications v1.3," , Oct. 2015.
[4] IEEE, "IEEE–part 11: Wireless LAN medium access control (MAC) and physical layer (PHY) specifications–amendment 4," http://ieeexplore.ieee.org/servlet/opac?punumber=6687185, 2013.
[5] W. Afifi and M. Krunz, "Exploiting self-interference suppression for improved spectrum awareness/efficiency in cognitive radio systems," in *Proc. of the IEEE INFOCOM'13 Conf.*, Apr. 2013, pp. 1258–1266.

[6] ——, "TSRA: An adaptive mechanism for switching between communication modes in full-duplex opportunistic spectrum access systems," *IEEE Transactions on Mobile Computing*, 2016.

[7] Huawei and U. of Electronic Science & Technology of China, "Sensing scheme for DVB-T," IEEE Std.802.22-06/0127r1, July. 2006.

[8] S. Chaudhari, V. Koivunen, and H. V. Poor, "Autocorrelation-based decentralized sequential detection of OFDM signals in cognitive radios," *IEEE Trans. Signal Process.*, vol. 57, no. 7, pp. 2690–2700, 2009.

[9] E. Axell and E. G. Larsson, "Optimal and sub-optimal spectrum sensing of OFDM signals in known and unknown noise variance," *IEEE J. Select Areas in Commun.*, vol. 29, no. 2, pp. 290–304, 2011.

[10] S. Biaz and S. Wu, "Rate adaptation algorithms for IEEE 802.11 networks: A survey and comparison," in *Proc. of IEEE ISCC '08 Symp.*, July 2008, pp. 130–136.

[11] A. W. Min and K. G. Shin, "An optimal transmission strategy for IEEE 802.11 wireless LANs: Stochastic control approach," in *Proc. of the IEEE SECON'08 Conf.*, June 2008, pp. 251–259.

[12] A. K. Karmokar, D. V. Djonin, and V. K. Bhargava, "POMDP-based coding rate adaptation for type-I hybrid ARQ systems over fading channels with memory," *IEEE Transactions on Wireless Communications*, vol. 5, no. 12, pp. 3512–3523, December 2006.

[13] D. V. Djonin, A. K. Karmokar, and V. K. Bhargava, "Joint rate and power adaptation for type-I hybrid ARQ systems over correlated fading channels under different buffer-cost constraints," *IEEE Transactions on Vehicular Technology*, vol. 57, no. 1, pp. 421–435, Jan 2008.

[14] V. Krishnamurthy, "Algorithms for optimal scheduling and management of hidden Markov model sensors," *IEEE Trans. Signal Process.*, vol. 50, no. 6, pp. 1382–1397, June. 2002.

[15] S. Sagari, S. Baysting, D. Saha, I. Seskar, W. Trappe, and D. Raychaudhuri, "Coordinated dynamic spectrum management of LTE-U and Wi-Fi networks," in *Proc. of the IEEE DySPAN'2015 Conf.*, Sept. 2015, pp. 209–220.

[16] Y. Li, F. Baccelli, J. G. Andrews, T. D. Novlan, and J. Zhang, "Modeling and analyzing the coexistence of licensed-assisted access LTE and Wi-Fi," in *Proc. of IEEE GC Wkshps'2015 Conf.*, Dec. 2015, pp. 1–6.

[17] O. Sallent, J. Perez-Romero, R. Ferrus, and R. Agusti, "Learning-based coexistence for LTE operation in unlicensed bands," in *Proc. of the IEEE ICC Wkshps'15 Conf.*, June 2015, pp. 2307–2313.

[18] H. Zhang, X. Chu, W. Guo, and S. Wang, "Coexistence of Wi-Fi and heterogeneous small cell networks sharing unlicensed spectrum," *IEEE Communications Magazine*, vol. 53, no. 3, pp. 158–164, March 2015.

[19] C. Cano and D. J. Leith, "Coexistence of WiFi and LTE in unlicensed bands: A proportional fair allocation scheme," in *Proc. of IEEE ICC Wkshps'15 Conf.*, June 2015, pp. 2288–2293.

[20] M. Hirzallah, W. Afifi, and M. Krunz, "Full-duplex spectrum sensing and fairness mechanisms for Wi-Fi/LTE-U coexistence," *Proc. of the IEEE GLOBECOM'16 Conf.*, 2016.

[21] ——, "Full-duplex adaptation strategies for Wi-Fi/LTE-U coexistence," University of Arizona, Department of ECE, TR-UA-ECE-2016-3, Tech. Rep., Nov. 2016. [Online]. Available: http://www2.engr.arizona.edu/~krunz/publications_by_type.htm#trs

[22] T. W. Hong and M. N., "Finite state Markov channel a useful model for radio communication channels," *IEEE Trans. Vehicular Technologies*, vol. 44, no. 1, pp. 163–171, Feb 1995.

[23] S. M. Ross, *Stochastic processes*, 2nd ed. John Wiley & Sons New York, 1996.

[24] A. Georgiadis, "Gain, phase imbalance, and phase noise effects on error vector magnitude," *IEEE Trans. Veh. Technol.*, vol. 53, no. 2, pp. 443–449, March 2004.

[25] R. D. Smallwood and E. J. Sondik, "The optimal control of partially observable Markov processes over a finite horizon," *Operations Research*, vol. 21, no. 5, pp. 1071–1088, 1973.

[26] G. Shani, J. Pineau, and R. Kaplow, "A survey of point-based POMDP solvers," *Auton. Agent. Multi-Agent Syst.*, vol. 27, pp. 1–51, 2013.

[27] S. Ross, J. Pineau, S. Paquet, and C.-D. B., "Online planning algorithms for POMDPs," *Journ. of Art. Int. Res.*, vol. 32, pp. 663–704, 2008.

[28] H. Kurniawati, D. Hsu, and W. Lee, "SARSOP: Efficient point-based POMDP planning by approximating optimally reachable belief spaces," in *Proc. Robotics: Science and Systems*, 2008.

Mohammed Hirzallah (S'15) received the B.Sc. degree in electrical engineering from the University of Jordan, Amman, Jordan, in 2011, and the M.Sc. degree in electrical and computer engineering from the University of Arizona, Tucson, AZ, in 2015. He is working toward his Ph.D. at the University of Arizona. Mohammed's research interests include the design and analysis of wireless protocols and systems. He investigates the problem of coexistence between heterogeneous wireless networks.

Wessam Afifi is working toward the PhD degree in the Department of Electrical and Computer Engineering, University of Arizona, and is a graduate research associate. In 2015, he was a wireless systems intern with Nokia Technologies, San Francisco. His research interests lie in the areas of wireless communications and networking, with emphasis on resource allocations, adaptive protocols, dynamic spectrum access systems, Wi-Fi/LTE-U coexistence, and full-duplex communications. He is a co-inventor of seven US patent applications and has published several peer-reviewed conference papers and journal articles. He has few contributions to the IEEE Standards. He won the first place in the graduate division of the physical sciences, mathematics, computer engineering, and computer science category for the student showcase, in Nov. 2014. In Jan. 2015, he won the GPSC Research and Project Grant. He won two best-poster awards at BWAC I/UCRCs in Apr. 2013 and Apr. 2016. He served as a TPC member and a reviewer for many conferences and journals.

Marwan Krunz is the Kenneth VonBehren Endowed Professor in the Department of ECE at the University of Arizona. He also holds a joint appointment as a professor of computer science. He co-directs the Broadband Wireless Access and Applications Center, a multi-university industry-focused NSF center that includes 16+ industry affiliates. He previously served as the UA site director for Connection One, an NSF IUCRC that focuses on wireless communication circuits and systems. He received his Ph.D. degree in electrical engineering from Michigan State University in 1995 and joined the University of Arizona in January 1997, after a brief postdoctoral stint at the University of Maryland. In 2010, he was a Visiting Chair of Excellence at the University of Carlos III de Madrid. He previously held various visiting research positions at University Technology Sydney, INRIA-Sophia Antipolis, HP Labs, University of Paris VI, University of Paris V, University of Jordan, and US West Advanced Technologies. Dr. Krunz's research interests lie in the areas of wireless communications and networking, with emphasis on resource management, adaptive protocols, and security issues. He has published more than 245 journal articles and peer-reviewed conference papers, and is a co-inventor on several US patents. He is an IEEE Fellow, an Arizona Engineering Faculty Fellow (2011-2014), and an IEEE Communications Society Distinguished Lecturer (2013 and 2014). He was the recipient of the 2012 IEEE TCCC Outstanding Service Award. He received the NSF CAREER award in 1998. He currently serves on the editorial board for the IEEE Transactions on Cognitive Communications and Networks. Previously, he served on the editorial boards for IEEE/ACM Transactions on Networking, IEEE Transactions on Mobile Computing (TMC), IEEE Transactions on Network and Service Management, Computer Communications Journal, and IEEE Communications Interactive Magazine. Effective January 2017, he will be the next EiC for TMC. He was the general vice-chair for WiOpt 2016 and general co-chair for WiSec'12. He was the TPC chair for WCNC 2016 (Networking Track), INFOCOM'04, SECON'05, WoWMoM'06, and Hot Interconnects 9. He has served and continues to serve on the steering and advisory committees of numerous conferences and on the panels of several funding agencies. He was a keynote speaker, an invited panelist, and a tutorial presenter at numerous international conferences. See http://www2.engr.arizona.edu/ krunz/ for more details.